R. Kotte, J. Biegansky, J. Mösner,
W. Neubert, C. Plettner, D. Wohlfahrt et al.
(FOPI Collaboration)

Proton-Proton Correlations in
Central Collisions of Ni+Ni at 1.93 A·GeV
and the Space-Time Extent
of the Emission Source

Forschungszentrum Rossendorf e.V.

Postfach 51 01 19 · D-01314 Dresden
Bundesrepublik Deutschland

Telefon	(0351) 260 2323
Telefax	(0351) 260 3700
E-Mail	kotte@fz-rossendorf.de

Proton-Proton Correlations in Central Collisions of Ni+Ni at 1.93 A·GeV and the Space-Time Extent of the Emission Source

FOPI Collaboration

R. Kotte[5], J. Biegansky[5], J. Mösner[5], W. Neubert[5], C. Plettner[5], D. Wohlfarth[5], J. P. Alard[3], V. Amouroux[3], Z. Basrak[11], N. Bastid[3], I. Belyaev[7], D. Best[4], A. Buta[1], R. Čaplar[11], N. Cindro[11], J. P. Coffin[9], P. Crochet[9], R. Dona[9], P. Dupieux[3], M. Dželalija[11], M. Eskef[6], P. Fintz[9], Z. Fodor[2], L. Fraysse[3], A. Genoux-Lubain[3], G. Göbels[6], A. Gobbi[4], G. Guillaume[9], E. Häfele[6], N. Herrmann[4,6], K. D. Hildenbrand[4], S. Hölbling[11], B. Hong[4], F. Jundt[9], J. Kecskemeti[2], M. Kirejczyk[4,10], M. Korolija[6], C. Kuhn[9], A. Lebedev[7], I. Legrand[1], Y. Leifels[4], C. Maazouzi[9], V. Manko[8], H. Merlitz[6], S. Mohren[6], D. Pelte[6], M. Petrovici[1], C. Pinkenburg[4], P. Pras[4], F. Rami[9], W. Reisdorf[4], J. L. Ritman[4], C. Roy[9], D. Schüll[4], Z. Seres[2], B. Sikora[10], V. Simion[1], K. Siwek-Wilczyńska[10], U. Sodan[4], A. Somov[7], L. Tizniti[9], M. Trzaska[6], M. A. Vasiliev[8], P. Wagner[9], G. S. Wang[4], T. Wienold[4], Y. Yatsunenko[7], and A. Zhilin[7]

[1] Institute for Nuclear Physics and Engineering, Bucharest, Romania
[2] Central Research Institute for Physics, Budapest, Hungary
[3] Laboratoire de Physique Corpusculaire, Université Blaise Pascal, Clermont-Ferrand, France
[4] Gesellschaft für Schwerionenforschung, Darmstadt, Germany
[5] Forschungszentrum Rossendorf, Dresden, Germany
[6] Physikalisches Institut der Universität Heidelberg, Heidelberg, Germany
[7] Institute for Experimental and Theoretical Physics, Moscow, Russia
[8] Kurchatov Institute for Atomic Energy, Moscow, Russia
[9] Centre de Recherches Nucléaires, Université Louis Pasteur, Strasbourg, France
[10] Institute of Experimental Physics, Warsaw University, Warsaw, Poland
[11] Rudjer Bošković Institute Zagreb, Zagreb, Croatia

Abstract. Small-angle correlations of proton pairs produced in central Ni+Ni collisions at a beam energy of 1.93 A·GeV are investigated with the FOPI detector system at GSI Darmstadt. A well-defined emission source is selected by triggering on central events which comprise about 8% of the total cross section. Simultaneous comparison of longitudinal and transverse correlation functions with the predictions of the Koonin model allows to unravel the space-time ambiguity of the emission process. Taking into account the strong collective expansion of the participant zone, which introduces a reduction of the extracted source radius of more than 30%, r.m.s. radius and emission time parameters of $R_{rms} = (4.2\pm1.2)$ fm and $t_{rms} = (11^{+7}_{-5})$ fm/c are extracted, respectively. In contrast, the analysis of the angle-integrated correlation function gives an upper limit $R_{rms} = (7.0 \pm 1.4)$ fm of the source radius.

PACS: 25.70.Pq

1 Introduction

Two-proton correlation functions at small relative momenta can probe the space-time extent of the reaction zone created in heavy-ion reactions. This is due to the fact that the magnitude of nuclear and Coulomb final-state interactions as well as antisymmetrization effects, depend on the spatial and temporal separation of the two protons [1-15]. Usually, the correlation functions are evaluated as a function of the relative

momentum $|q| = \frac{1}{2}|p_1 - p_2|$. The attractive s-wave nuclear interaction leads to a maximum in the correlation function at $q \sim 20$ MeV/c, whereas Coulomb repulsion and antisymmetrization cause a minimum at $q = 0$ [1, 7]. Most analyses give only upper limits for the spatial extent of the source because of an ambiguous interplay of radius and lifetime of the source. Thus, model calculations simulating large sources with short lifetimes can lead to similar correlation functions as model calculations simulating small sources with long lifetimes [1, 6]. This ambiguity may be avoided by applying cuts on the angle between the vectors of the relative momentum q and the total pair momentum $P = p_1 + p_2$ [1, 3, 6, 11, 15].

For a source of finite lifetime τ, the phase space distribution of the emitted protons is elongated in the direction of P by $\langle v \rangle \tau$, where $\langle v \rangle$ is the emission velocity of the pair. For such distributions, the Pauli suppression due to the antisymmetrization of the wave functions is smaller in the elongated (longitudinal, $q \| P$) direction as compared to the nonelongated (transverse, $q \perp P$) direction. Reliable impact parameter sampling is needed for the selection of well-defined sources, where certain longitudinal and transverse cuts can be applied in the source rest frame. Otherwise, the small effect of the directional dependence (about 5-10% of the height of the the correlation peak [13]) will be washed out.

2 The experiment

The experiment has been performed at the heavy-ion synchrotron SIS at GSI Darmstadt. A ^{58}Ni target of 1% interaction thickness has been irradiated by ^{58}Ni ions of 1.93 A·GeV beam energy. The present analysis uses a subsample of the data, taken with the outer Plastic Wall/Helitron combination

(which covers polar angles from 8.5 to 26.5 degrees) of the FOPI detector system [16]. The Plastic Wall delivers - via energy loss vs. time-of-flight (TOF) measurement - the nuclear charge Z and the velocity β of the particles. The Helitron [17] gives the curvature (which is a measure of the momentum over charge (p/Z)) of the particle track in the field of a large superconducting solenoid. Since the momentum resolution of the Helitron is rather moderate, this detector component serves for particle identification only. The mass m is determined via $mc = (p/Z)_{Hel}/(\beta\gamma/Z)_{PlaWa}$ where $\gamma = (1 - \beta^2)^{-1/2}$. Protons are selected by setting a gate of $\Delta m = \pm 0.30$ GeV/c^2 on the corresponding mass peak which has a width of about 0.29 GeV/c^2 FWHM (0.86 GeV/c^2 FWTM). Contaminations of π^+ mesons can be neglected since they exhibit a well separated mass peak with a width of 0.09 GeV/c^2 FWHM (0.23 GeV/c^2 FWTM) whereas contributions of π^- mesons are almost excluded due to the inverse deflection in the magnetic field. From the velocity, which is measured with a resolution[1] of about 2% (FWHM), other kinetic quantities like the proton momenta are deduced.

Fig. 1 shows the phase space coverage of the detector components outer Plastic Wall/Helitron in the transverse momentum vs. rapidity plane for a central source distribution. Here, for illustrative purposes the source is simply modelled by a three-dimensional Gaussian in momentum space with dispersion $\sigma^2(p^o) = 1/8$. Reduced quantities $p^o = (p/A)/(p/A)^{cm}_{proj} = (\beta\gamma)/(\beta\gamma)^{cm}_{proj}$ and $y^o = y/y_{cm} - 1$ are used (where $y_{cm} = 0.89$ and $(p/A)^{cm}_{proj} = 0.951$ GeV/c for symmetric collisions at 1.93 A·GeV projectile energy). The indicated lines of constant reduced momentum p^o of 0.14, 0.47 and 1.00 correspond to c.m. kinetic energies of 0.01, 0.1 and 0.4 A·GeV, respectively. It is obvious that for central collisions the Plastic Wall preferentially measures midrapidity particles with small momenta.
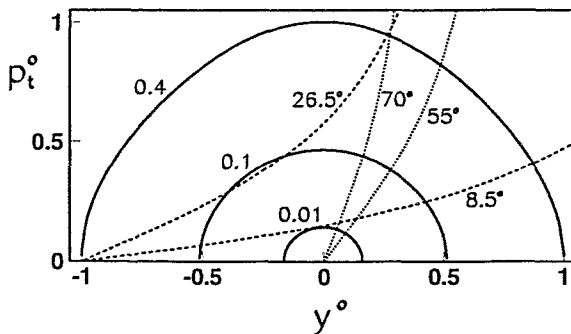
3 Event classification

Central collisions are selected with the online condition "central trigger" (about 10^6 events) as well as by cutting on large values of the ratio $E_{rat} = \sum_i E_{\perp i}/\sum_i E_{\|i}$ of total transverse and longitudinal kinetic energies [18] calculated in the forward c.m. hemisphere within $1^o < \theta_{lab} < 30^o$.

Fig. 2 displays the multiplicity distribution of charged particles measured in the outer Plastic Wall (cf. Fig. 1). The corresponding integrated cross sections are indicated for different trigger conditions. A maximum impact parameter of $b_{max} = 9.3$ fm is assumed which corresponds to a total cross section of 2700 mb. Integrated cross sections of about 8% and 2% of the total one are selected with the central trigger and the E_{rat} conditions, respectively. For these centrality classes one would expect - within a geometrical picture - an average impact parameter of about 1.8 fm and 0.9 fm. Simulations which we have performed with the IQMD model [19] predict an average impact parameter of about 2 fm for the 220 mb multiplicity cut. For very central collisions the E_{rat} quantity is found slightly better correlated with impact parameter than the charged particle multiplicity. Thus, an average impact parameter of about 1.3 fm (1.5 fm) is predicted for the 55 mb E_{rat} (multiplicity) cut. Furthermore, the IQMD simulations have shown that at very low multiplicities the PMUL distribution decreases slightly steeper than the exponential fall-off (dashed line in Fig. 2) which is assumed in the region of unmeasured multiplicities. Consequently, the numbers attributed to the central cuts represent upper limits of the integrated cross sections.
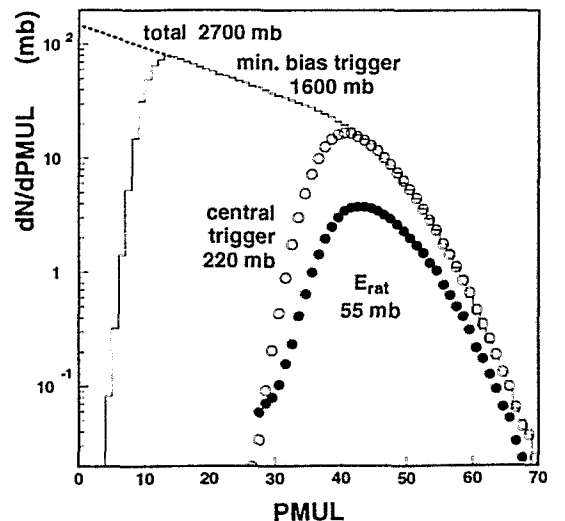

Fig. 1. Contour plot of invariant cross section $d^2\sigma/p_t\,dp_t\,dy$ in the $p_t^o - y^o$ plane of a central model source simulated by a three-dimensional Gaussian. The full lines are levels of constant yield of 2, 42 and 92 % of the maximum value. The corresponding c.m. kinetic energies of 0.01, 0.1 and 0.4 GeV per nucleon are indicated. Dashed lines represent the polar angle limits at 8.5 and 26.5 degrees. Dotted lines give c.m. polar angles of 55 and 70 degrees.

Fig. 2. Distribution of charged particle multiplicity PMUL measured in the outer Plastic Wall of FOPI. The histogram shows the distribution for the minimum bias condition. The open dots represent the event distribution for the central trigger. Full dots are events selected by cutting on high values of the ratio E_{rat} of total transverse and longitudinal energies. The dashed line approximates the shape of the distribution of not recorded low multiplicities which is extrapolated assuming an exponential spectral shape.

_____

[1] Taking into account that all particles of an event suffer from the same time jitter of the start detector, two-particle quantities like the relative momenta of proton pairs are even less affected by the TOF resolution.

In a previous investigation of central Au+Au collisions between 100 and 400 A·MeV beam energy it was found that

the correlation function of pairs of intermediate mass fragments (IMF) is strongly affected by the collective directed sideward flow of nuclear matter [20, 21]. This directed sideflow causes an enhancement of correlations at small relative momenta. The enhancement results from mixing of differently azimuthally oriented events; it vanishes if the events are rotated into a unique reaction plane [22]. Therefore, the technique of event rotation is applied to the data in order to exclude such dynamical correlations. Since the protons are more isotropically distributed in phase space as compared to heavier clusters (like helium fragments, see Fig. 3) the effect is expected to be small.
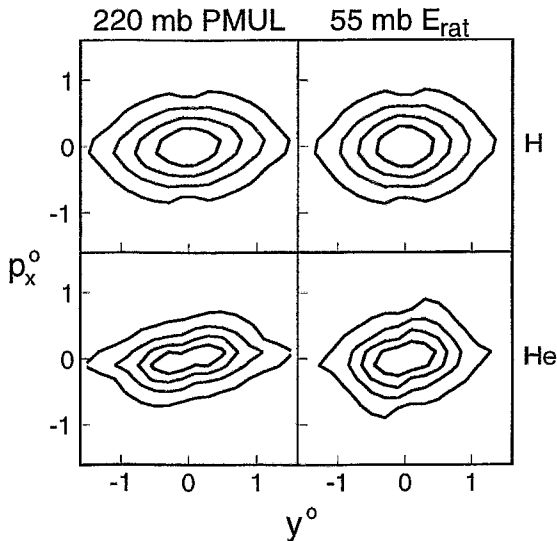

Fig. 3. Two-dimensional distribution of particle yields $d^2N/dp_x\,dy$ in the plane of reduced transverse momentum (projected onto the reaction plane) vs. normalized rapidity of hydrogen (mostly protons, upper part) and helium (mostly ^3He, lower part) fragments measured with the whole forward wall. The isolines are given for 20, 40, 60, and 80% of the maximum value. The left column shows the distributions for the central trigger condition. The right column represents the events selected by cutting on high values of the ratio E_{rat} of total transverse and longitudinal energies. The measured data of the forward hemisphere are reflected to the backward one.

4 The correlation function

Let $Y_{12}(\mathbf{p}_1, \mathbf{p}_2)$ be the coincidence yield of proton pairs. Then the two-particle correlation function is defined as

$$1 + R(\mathbf{p}_1, \mathbf{p}_2) = \mathcal{N}\,\frac{\sum_{events,pairs} Y_{12}(\mathbf{p}_1, \mathbf{p}_2)}{\sum_{events,pairs} Y_{12,mix}(\mathbf{p}_1, \mathbf{p}_2)}. \qquad (1)$$

The sum runs over all events fulfilling the above mentioned global selection criteria and over all pairs satisfying certain conditions given below. Event mixing, denoted by the subscript "mix", means to take particle #1 and particle #2 from different events. We only mix events found within the same event class. $\mathcal{N}$ is a normalization factor fixed by the requirement to have the same number of true and mixed pairs. The correlation function (1) is than projected onto the relative momentum

$$q = |\mathbf{q}| = |\mathbf{p}_1 - \mathbf{p}_2|/2. \qquad (2)$$

Besides the above described global event characteristics we use gate conditions on the angle α between $\mathbf{q}$ and the c.m. sum momentum of the proton pair $\mathbf{P}_{12}^{cm} = \mathbf{p}_1^{cm} + \mathbf{p}_2^{cm}$ and on the normalized pair momentum $p_{12}^o = |\mathbf{P}_{12}^{cm}|/(2 \cdot (p/A)_{proj}^{cm})$.

5 Results and comparison with model

Fig. 4 shows the two-proton correlation function and the relative momentum distribution of proton pairs from collisions selected with the central trigger condition. The dashed line in the lower part represents the distribution of the uncorrelated background which is produced with the event mixing technique. The statistical errors of all the correlation functions presented here are governed by those of the coincidence yield, since the mixed yield is generated with two orders of magnitude higher statistics.
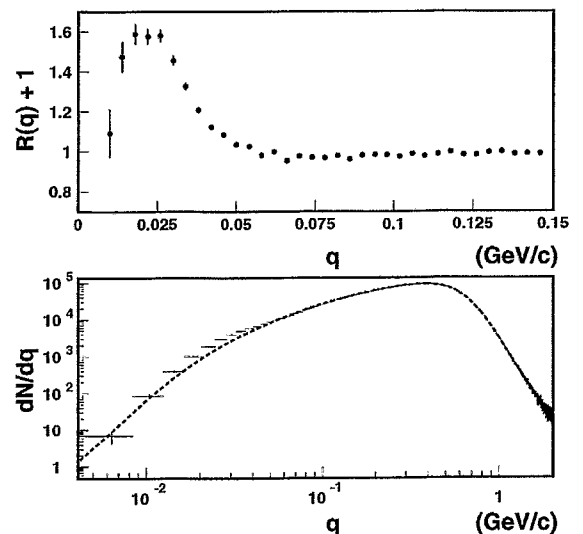

Fig. 4. The experimental relative momentum yield (lower part) and the corresponding correlation function (upper part) of proton pairs from central trigger events. The dashed line represents the uncorrelated background which is constructed via event mixing.

Obviously, the correlation peak is dominated by the contribution of very few proton pairs in the relative momentum range 10 MeV/c $< q <$ 50 MeV/c which show up above the background distribution. The corresponding yield is less than 1 per thousand. For large relative momenta the mixed yield coincides perfectly with the coincidence yield. Consequently, a normalization procedure where the constant $\mathcal{N}$ in Eq. (1) is determined by the requirement that $R(q)$ vanishes for large q (cp. refs. [10-13]) would give the same correlation function.

As in previous fragment-fragment correlation analyses [20, 21] an enhanced coincidence yield at very small relative angles is observed, which is due to double counting caused partially by the tiny geometrical overlap of two plastic scintillators and mainly by scattering in the scintillator strips. This disturbing yield is reduced drastically by the requirement to match the particle hits on the Plastic Wall with the

corresponding tracks in the forward drift chamber Helitron. However, mismatches of tracks and scattering processes especially at the wire planes of the chamber can give rise to a small amount of double counting, too. The remaining small amount of pairs of doubly counted particles is eliminated by excluding, around a given hit, positions within a rectangular segment of $|\phi_1 - \phi_2| < 4^o$ and $|\theta_1 - \theta_2| < 2^o$. The relative-momentum distribution of the excluded proton pairs allows for a direct experimental determination of the q resolution. For the dispersion of this distribution a typical value of $\sigma_{exp}(q) \simeq (6 \pm 1)$ MeV/c is estimated. In order to keep the influence of the exclusion of small angles onto the correlation function as small as possible, the same procedure is applied to the uncorrelated background. Additionally, the bias of the correlation function at very small relative momenta due to the exclusion procedure is tested with GEANT [23] simulations using the IQMD model [19] as event generator. It has been found that for $q > 12$ MeV/c the correlation peak, which is a measure of the source size, is almost unbiased.

Fig. 5 shows two-proton correlation functions of central events selected by the central trigger (dots) and by the 55 mb E_{rat} condition (squares). No variation of the correlation with increasing centrality is observed. This is not surprising since the phase space distribution of protons changes only slightly with decreasing cross section whereas that of the heavier fragments shows a significant evolution to a much more compact central source (cf. Fig. 3). Therefore, we restrict ourselves to the more abundant central trigger data which would allow additional cuts on the normalized pair momentum p_{12}^o and on the angle α between the sum and the difference of the momenta of the proton pairs (cf. Section 4).

is somewhat in contrast to the strong increase of the correlation peak with the total pair momentum found for central collisions of Ar+Sc at 80 $A\cdot$MeV, where also Boltzmann-Uehling-Uhlenbeck (BUU) calculations predict not only the same trend but also the same magnitude of the effect [10, 13]. Unfortunately, we can access only a momentum range restricted to $p_{12}^o < 0.8$ (cf. Fig. 1) due to the necessity of having a sufficiently large number of pairs with small relative momenta. On the other hand, the restriction to small c.m. momenta should have the advantage of carrying an increased sensitivity to lifetime effects [11, 13, 15] when applying directional cuts on the correlation function (see below).

In Fig. 6 the angle-integrated two-proton correlation function of central trigger events is compared with the prediction of the Koonin model [1] with zero lifetime and Gaussian radius $R_o = \sqrt{\frac{2}{3}}R_{rms} = (3.9 \pm 0.8)$ fm. The theoretical correlation function is folded with different q resolutions $\sigma_{exp}(q)$. The following observations have to be pointed out: Only with the resolution of $\sigma_{exp}(q) = 6$ MeV/c (full line) the folded Koonin curve reproduces the shape of the experimental correlation function. The dotted and dashed-dotted lines should give an impression of the typical variation of the peak height with the resolution. This variation corresponds to a variation of the r.m.s. radius of about ± 0.2 fm. Without taking into account the experimental resolution (dashed line) at all the height (width) of the peak would be higher (smaller) than the experimental one. A 10% larger source radius ($R_{rms} \simeq 5.3$ fm) would be necessary in the Koonin model in order to match the experimental peak height.
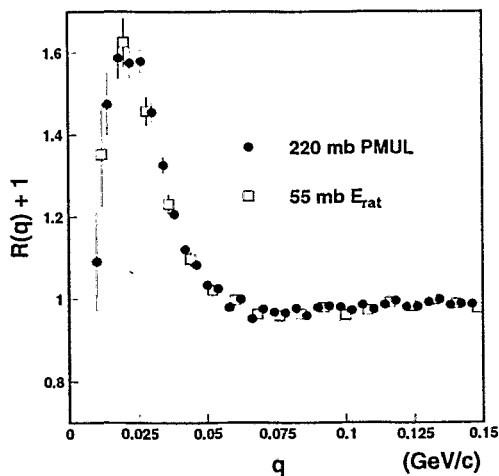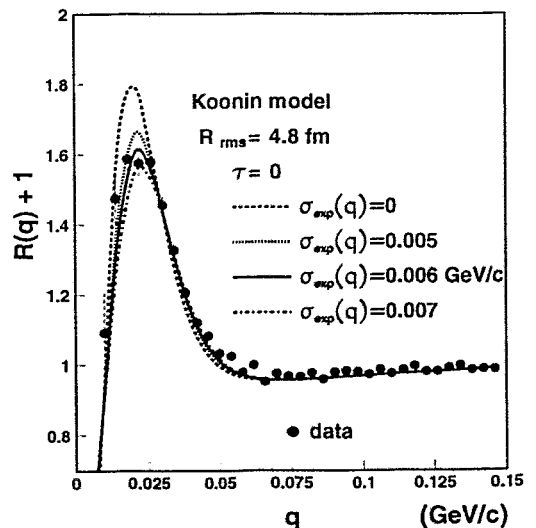

Fig. 5. Correlation functions of proton pairs selected with the central trigger condition (full dots) and with a 55 mb cut on large values of the ratio E_{rat} of total transverse and longitudinal energies (open squares).

Fig. 6. Correlation functions of proton pairs selected with the central trigger condition (dots). The different lines are results of Koonin model simulations with zero lifetime τ and Gaussian radius $R_o = \sqrt{\frac{2}{3}}R_{rms}$ folded with an experimental resolution function of Gaussian shape with different dispersions $\sigma_{exp}(q)$.

No significant dependence of the correlation peak on the pair momentum has been observed. The averaged (over a relative momentum region of $q = 12 - 32$ MeV/c) peak height rises only by 1% if the normalized momentum is increased from $p_{12}^o = 0.3 \pm 0.1$ to $p_{12}^o = 0.7 \pm 0.1$. (Simultaneously, the statistical error increases from 2% to 4%.) This finding

The space-time ambiguity of the correlation function can be reduced by analysing two-proton correlations with cuts on the angle $\alpha = cos^{-1}(\mathbf{P} \cdot \mathbf{q}/(Pq))$ between $\mathbf{P}$ and $\mathbf{q}$. As mentioned in Section 1, the correlation function carries a di-

rectional sensitivity due to the Pauli suppression in the non-elongated direction [1, 6]. Since the pair momentum **P** depends on the rest frame of the source, whereas the relative momentum **q** does not[2], the angle α depends on the rest frame of the emitting source. Thus, a careful selection of a well-defined emission source is required. In the present analysis, we investigate correlation functions of proton pairs from central trigger events. The pair momentum is defined in the rest frame of the central source, $\mathbf{P} \equiv \mathbf{P}_{12}^{cm}$. Experimental transverse and longitudinal correlation functions are generated here by selecting proton pairs with angles $|cos(\alpha)| < 0.5$ and $|cos(\alpha)| > 0.5$, respectively[3]. These cuts are applied both to the coincidence yield and to the uncorrelated background. The normalization constant $\mathcal{N}$ in Eq. (1) is determined individually for each α cut. The longitudinal and transverse correlation functions are presented in Fig. 7. The wanted effect

width of the correlation peak. Thus, the experimental resolution even increases the difference of the peak heights and consequently the sensitivity of the directional cuts to possible lifetime effects. Koonin model calculations of longitudinal and transverse p-p correlations are performed for a wide range of Gaussian source parameters R_o and $\langle v \rangle \tau$. The results of the model are folded with the experimental resolution of $\sigma_{exp}(q) = 6$ MeV/c. In order to find the optimum set of parameters, for each set the agreement between experimental and simulated transverse and longitudinal correlation functions is tested by evaluating the χ^2 per degree of freedom in the peak region of $q = 12 - 32$ MeV/c (5 bins each 4 MeV/c wide). Fig. 8 shows, as contour plot, the distribution of this quantity as function of R_{rms} and $\langle v \rangle \tau$.
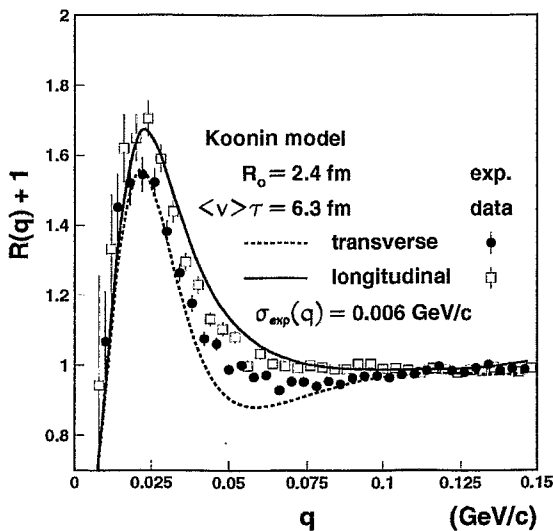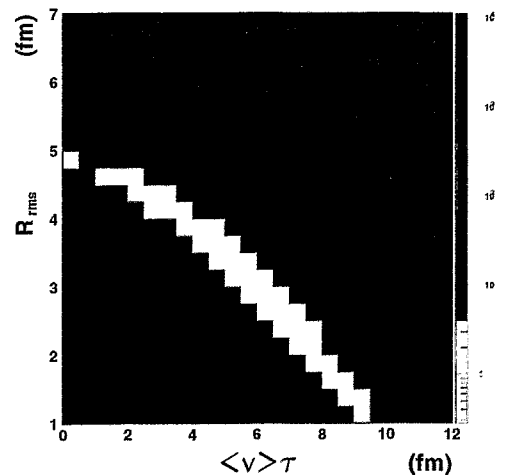

Fig. 7. Transverse (dots) and longitudinal (squares) correlation functions of proton pairs selected with the central trigger condition. Dashed and full lines are the corresponding results of Koonin model calculations using the Gaussian source parameters of radius and lifetime $R_o = 2.4$ fm and $\langle v \rangle \tau = 6.3$ fm, respectively, as delivered by the χ^2 minimum of Fig. 8. The results of the model are folded with an experimental resolution of $\sigma_{exp}(q) = 6$ MeV/c.

Fig. 8. The distribution of χ^2 per degree of freedom as determined by simultaneously comparing measured longitudinal and transverse correlation functions (over the range $q = 12 - 32$ MeV/c) with the correlation functions predicted by the Koonin model. The quantity is given in dependence of the r.m.s. radius R_{rms} and the Gaussian lifetime parameter $\langle v \rangle \tau$.

is clearly visible: We find a suppression of the transverse correlations with respect to the longitudinal ones of about 10% which is consistent with model predictions for the emission from a source of finite lifetime [1, 3, 6]. Obviously, the peak width of the transverse correlation function is smaller than the width of the longitudinal one. The finite q resolution leads to a reduction of the height and an increase of the

The best agreement of experimental data and model calculations is found for Gaussian source parameters of $R_o = (2.35 \pm 0.65)$ fm and $\langle v \rangle \tau = (6.3 \pm 1.7)$ fm. The corresponding r.m.s. quantities are $R_{rms} = \sqrt{3/2}R_o = (2.9 \pm 0.8)$ fm and $\langle v \rangle t_{rms} = \langle v \rangle \tau / \sqrt{2} = (4.5 \pm 1.2)$ fm. The results of the Koonin model with this parameter set are depicted in Fig. 7. It should be mentioned that for zero lifetime in Fig. 8 one would predict an r.m.s. radius of $R_{rms} = 4.9$ fm in good agreement with the results of the previous analysis of the angle-integrated correlation function (cp. Fig. 6). For the determination of the mean lifetime of the emission process one has to take into account the emission velocity of the particles. For proton pairs of central trigger events, which have relative momenta in the region of the correlation peak, this velocity exhibits a distribution with a mean value $\langle v \rangle = 0.42$ c and a dispersion $\sigma_v = 0.1$ c. Considering these quantities an r.m.s. lifetime of $t_{rms} = (11^{+7}_{-5})$ fm/c can be derived.

The present source emission time is only slightly larger than the total transit time $t_{tr} \simeq 6$ fm/c of the colliding nuclei. Furthermore, it does well compare with results of calculations we have performed with the BUU model [24] which predict

---

[2] For the present system and phase space coverage the Lorentz invariant momentum difference q_{inv} deviates by less than 5% from the classical momentum difference q as far as one deals with momenta in the c.m. system of the source. This deviation vanishes for true transverse correlations (since the particles have the same energy) and it is largest for true longitudinal correlations (which cannot be measured due to the finite granularity of the detector system).

[3] More restrictive conditions as $|cos(\alpha)| < 0.26$ and $|cos(\alpha)| > 0.64$ for the selection of transverse and longitudinal correlations lead to the same results.

about 10 fm/c for the time the system needs for the expansion from the maximum density of about two times nuclear matter ground state density $\rho \simeq 2\rho_o$ to a value of $\rho \simeq \rho_o/4$.

Since central nucleus-nucleus collisions are characterized by the collective expansion of nuclear matter after the compression phase the question arises how the extracted source radii are influenced by this correlation of coordinate and momentum space. For this reason, we have modified within the Koonin model the single-proton phase space emission function

$$g(\mathbf{p}, \mathbf{r}, t) \propto \exp\left(-\frac{p^2}{2m_pT} - \frac{r^2}{R_o^2} - \frac{t^2}{\tau^2}\right) \qquad (3)$$

by introducing a linear velocity profile which accounts for the radial expansion

$$\exp\left(-\frac{p^2}{2m_pT}\right) \longrightarrow \exp\left(-\frac{(\mathbf{p} - \alpha\mathbf{r})^2}{2m_pT}\right). \qquad (4)$$

Repeating the derivation given in ref. [1] (see also ref. [7]) one gets the same relation for the correlation function $C(\mathbf{P}, \mathbf{q}) = 1 + R(\mathbf{P}, \mathbf{q})$ containing a reduced radius

$$R^* = \frac{R_o}{\sqrt{1 + \frac{2}{3}\frac{E_r}{T}}} \qquad (5)$$

instead of the original source radius R_o. The parameter α is connected with the (non-relativistic) radial flow energy

$$E_r \equiv \frac{m_pc^2\beta_r^2}{2} = \frac{\langle\alpha^2 r^2\rangle}{2m_p} = \frac{3}{4}\frac{\alpha^2 R_o^2}{m_p} \qquad (6)$$

and with the mean radial blast velocity β_r whereas m_p and T represent the proton mass and the temperature, respectively. (The brackets in Eq. (6) imply averaging over the Gaussian density distribution.) From Eq. (5) one finds that the apparent source radius R^* decreases monotonously with increasing ratio of flow energy over temperature and that the relative reduction R^*/R_o does not depend on the radius itself. These observations do well compare with recent results of the investigation of the sensitivity of the proton-proton correlation to collective expansion in central Au+Au collisions at 150.4·MeV beam energy [25]. There, the authors performed schematic calculations based on the Pratt [2, 5, 6] formalism using a homogeneously filled sphere and a self-similar velocity profile superimposed on the thermal velocity distribution. They find a relative reduction of the source radius of about 15% - 20% if radial flow energies and temperatures comparable to the experimental findings [18, 26] are taken into account. A very similar radius correction would be calculated with Eq. (5). In contrast, the apparent reduction of the source radius due to radial expansion as deduced from relative-velocity correlations of IMF pairs in case of central Au+Au reactions between 100 and 400 A·MeV [20, 21] is much stronger (up to a factor of two). This can be attributed to the fact that heavy fragments probe collective motion effects more sensitively than light particles [26].

For the quantitative estimate of the apparent reduction of the present source radius due to collective expansion we have generated energy distributions of light charged particles measured with the same Plastic Wall/Helitron detector combination as used for the investigation of the two-proton correlations. Proton, deuteron and triton c.m. kinetic energy

spectra have been accumulated in the polar angle range of $55° < \Theta_{cm} < 70°$ (cf. Fig. 1). They are analysed in the framework of the picture which assumes that the final energy distribution is the result of the superposition of a collective expansion and a random thermal motion. Using the relativistic form [28]

$$\langle E_k\rangle = A(\frac{E}{A})_{flow} + \gamma_r\left(Am_0\left[\frac{K_1(Am_0/T)}{K_2(Am_0/T)} - 1\right] + 3T\right)(7)$$

of the dependence of the mean kinetic energy $\langle E_k\rangle$ on the mass number A (where $\gamma_r = (1 - \beta_r^2)^{-1/2}$ and K_J is the modified Bessel function of order J), a temperature of $T = (72 \pm 8)$ MeV and a flow energy per nucleon of $(\frac{E}{A})_{flow} = m_0(\gamma_r - 1) = (138 \pm 12)$ MeV are deduced[4]. In addition, a simultaneous fit of the shape of the three spectra with the Siemens-Rasmussen formula [29, 28] of an expanding spherical shell has been performed. From this analysis we get the very similar results $T = (65 \pm 8)$ MeV and $(\frac{E}{A})_{flow} = (138 \pm 13)$ MeV. The deduced (relativistic) flow energy is equivalent to an averaged expansion velocity of $\beta_r \simeq 0.49$[5]. Putting this blast velocity in Eq. (6) and taking an averaged temperature of $T = 68$ MeV the correction factor (square root in Eq. (5)) amounts to 1.45 ± 0.05 and gives a true r.m.s. radius of $R_{rms} = (4.2 \pm 1.2)$ fm. Similarly, the radius deduced from the angle-integrated correlation function has to be corrected to $R_{rms} = (7.0 \pm 1.4)$ fm.

6 Summary

In conclusion, we have presented experimental two-proton correlation functions for central collisions of Ni+Ni at 1.93 A·GeV.

For the first time the difference between transverse and longitudinal correlations has been derived in heavy-ion reactions at energies in the $1 - 2.4$·GeV region. This difference can be explained as a result of the finite source lifetime. The additional information allows to unravel the space-time ambiguity of the emission process. We have fitted simultaneously the longitudinal and transverse correlation functions with the predictions of the Koonin model taking into account the experimental relative-momentum resolution and the apparent reduction of the source radius due to collective expansion effects. The best agreement with experiment is obtained with r.m.s. parameters of the radius and the emission time of the source of $R_{rms} = (4.2 \pm 1.2)$ fm and $t_{rms} = (11^{+7}_{-5})$ fm/c, respectively. The corresponding sharp-sphere radius $R_{ss} = \sqrt{5/3}R_{rms}$ allows to determine the breakup volume $V = A/\rho = 4\pi R_{ss}^3/3 = 670$ fm^3 of the source. For

---

[4] The application of Eq. (7) in the non-relativistic limit $\langle E_k\rangle = A(\frac{E}{A})_{flow} + \frac{3}{2}T$ would give a very similar flow energy $(\frac{E}{A})_{flow} = (134 \pm 12)$ MeV but a significantly larger temperature $T = (93 \pm 10)$ MeV.

[5] Recently, transverse momentum distributions of π^-, p, d particles of central Au+Au and Ni+Ni collisions between 1 and 2 GeV per nucleon have been analysed in the framework of an expanding thermal source [27]. For the Ni+Ni system at 1.93 A·GeV the spectra of midrapidity particles with transverse momenta beyond the acceptance of the detector components used in the present pp-correlation analysis ($p_t^0 > 0.7$, cp. Fig. 1) give a temperature and a radial blast velocity of $T = (92 \pm 12)$ MeV and $\beta_r = 0.32 \pm 0.04$, respectively. The obvious observation of a longitudinally elongated proton momentum distribution is supported by the ellipsoidal flow patterns given in Fig. 3.

an estimated participant multiplicity of the central source of $A \simeq 80$ this volume gives a density of $\rho = 0.70\rho_o$.

In contrast, the usual comparison of the angle-integrated correlation function with the model mixes the spatial and temporal size of the source and delivers - after correcting for collective expansion - an upper limit $R_{rms} = (7.0 \pm 0.7)$ fm of the source radius. It would give a breakup volume (density) which is about 4.5 times larger (smaller) than the value delivered by the correlation function with directional cuts.

The estimated characteristic source emission time is the shortest one determined with the method of directional cuts on the two-proton correlation function known so far. It is only slightly larger than the transit time of the colliding nuclei and does well compare with the typical expansion time of the source. Thus, it is certainly appropriate to assume that the proton emission is not governed by sequential decay chains but by a sudden explosion/expansion process. Dealing with such short time scales the notation "lifetime" looses almost its meaning.

References

1. S.E. Koonin, Phys. Lett. **70B**, 43 (1977)
2. S. Pratt, Phys. Rev. Lett. **53**, 1219 (1984)
3. S. Pratt and M.B. Tsang, Phys. Rev. C **36**, 2390 (1987)
4. P. Dupieux et al., Phys. Lett. B **200**, 17 (1988)
5. W.G. Gong et al., Phys. Rev. Lett. **65**, 2114 (1990)
6. W.G. Gong, W. Bauer, C.K. Gelbke and S. Pratt, Phys. Rev. C **43**, 781 (1991)
7. W. Bauer, C.K. Gelbke and S. Pratt, Ann. Rev. Nucl. Part. Sci. **42**, 77 (1992), and references cited therein
8. W. Bauer, Nucl. Phys. **A545**, 369c (1992)
9. G.J. Kunde et al., Phys. Rev. Lett. **70**, 2545 (1993)
10. M.A. Lisa et al., Phys. Rev. Lett. **70**, 3709 (1993)
11. M.A. Lisa et al., Phys. Rev. Lett. **71**, 2863 (1993)
12. M.A. Lisa et al., Phys. Rev. C **49**, 2788 (1994)
13. D.O. Handzy et al., Phys. Rev. C **50**, 858 (1994)
14. T.S. Awes et al., Phys. Rev. Lett. **61**, 2665 (1988)
15. M. Korolija et al., Phys. Rev. Lett. **67**, 572 (1991)
16. A. Gobbi et al., FOPI collaboration, Nucl. Instr. Meth. **A324**, 156 (1993); J. Ritman for the FOPI collaboration, Nucl. Phys. (Proc. Suppl.) **B44**, 708 (1995)
17. Y. Leifels, GSI-Nachrichten, GSI 08-95, 4 (1995); S. Mohren et al., GSI Scientific Report 1995, GSI 96-1, 183 (1996)
18. S.C. Jeong et al., FOPI collaboration, Phys. Rev. Lett. **72**, 3468 (1994)
19. S.A. Bass, C. Hartnack, H. Stöcker and W. Greiner, Phys. Rev. C **51**, 3343 (1995)
20. B. Kämpfer et al., FOPI collaboration, Phys. Rev. C **48**, R955 (1993)
21. R. Kotte et al., FOPI collaboration, Phys. Rev. C **51**, 2686 (1995)
22. P. Danielewicz and G. Odyniec, Phys. Lett. **157B**, 146 (1985)
23. R. Brun, F. Bruyant, M. Maire, A.C. McPherson and P. Zanarini, GEANT3, CERN Data Handling Division, DD/EE/84-1, 10.1987
24. Gy. Wolf, W. Cassing, U. Mosel, Nucl. Phys. **A552**, 549 (1993), Phys. Lett. **271B**, 43 (1991); Gy. Wolf, G. Batko, W. Cassing, U. Mosel, K. Niita and M. Schäfer, Nucl. Phys. **A517**, 615 (1990)
25. H. Xi, ALADIN collaboration, GSI Scientific Report 1995, GSI 96-1, 37 (1996), GSI Nachrichten, GSI 01-96, 8 (1996)
26. W. Reisdorf et al., FOPI collaboration, "Central collisions of Au on Au at 150, 250 and 400 A-MeV", Nucl. Phys. A, in press
27. B. Hong et al., FOPI collaboration, "Stopping and Radial Flow in Central Nucleus-Nucleus Collisions between 1 and 2 GeV per Nucleon", to be published
28. G. Poggi et al., FOPI collaboration, Nucl. Phys. **A586**, 755 (1995)
29. P.J. Siemens and J.O. Rasmussen, Phys. Rev. Lett. **42**, 880 (1979)